Technical note: Testing a new approach for the determination of N_2 fixation rates by coupling a membrane equilibrator to a mass spectrometer for long term observations

Sören Iwe[1], Oliver Schmale[1], Bernd Schneider[1]

[1]Department of Marine Chemistry, Leibniz Institute for Baltic Sea Research Warnemünde (IOW), Rostock, 18119, Germany

Correspondence to: Sören Iwe (soeren.iwe@io-warnemuende.de), Oliver Schmale (oliver.schmale@io-warnemuende.de)

Abstract. Nitrogen fixation by cyanobacteria plays an important role in the eutrophication of the Baltic Sea, since it promotes biomass production in the absence of dissolved inorganic nitrogen (DIN). However, the estimates of the contribution of N_2 fixation to the N budget show a wide range. This is due to interannual variability, significant uncertainties in the various techniques used to determine N_2 fixation and in extrapolating local studies to entire basins. To overcome some of the limitations, we introduce a new approach using a Gas Equilibrium – Membrane-Inlet Mass Spectrometer (GE-MIMS). A membrane contactor (Liquicel) is utilized to establish gas phase equilibrium for atmospheric gases dissolved in seawater. The mole fractions for N_2, Ar and O_2 in the gas phase are determined continuously by mass spectrometry and yield the concentration of these gases by multiplication with the total pressure and the respective solubility constants. The results from laboratory tests show that the accuracy (deviation from expected values): N_2: 0.20 %, Ar: 0.70 %, O_2: 0.20 %, and the precision (2 times the absolute standard deviation) N_2: 0.05 %, Ar: 0.14 %, O_2: 0.11 % are sufficient enough to quantify the surface water N_2 depletion caused by N_2 fixation and to account for the interfering gas exchange on the basis of changes in the Ar concentration. The *e*-folding equilibration time is 4.8 min for N_2, 3.0 min for Ar and 3.2 min for O_2. Our GE-MIMS approach is designed for long-term observations on various platforms such as voluntary observing ships (VOS). The latter are particularly suited to achieve the temporal and spatial resolution necessary for studying large scale N_2 fixation in regions such as the Baltic Sea.

1 Introduction

Measuring the levels of dissolved gases such as CO_2, O_2 and N_2 in seawater is an established approach to investigate the biogeochemical processes associated with the production or decomposition of organic matter (OM). It is particularly well suited for monitoring coastal waters and semi-enclosed seas such as the Baltic Sea, where excessive nutrient inputs from river water and atmospheric deposition often lead to increased OM production (eutrophication). In the Baltic Sea, nitrogen fixation by cyanobacteria utilizing molecular nitrogen dissolved in surface water in the absence of dissolved inorganic nitrogen (DIN) can further amplify OM production.

These biogeochemical processes are linked to changes in the concentrations of dissolved atmospheric gases, and specifically the consumption and production of CO_2 and O_2, respectively, during net community production (NCP) and N_2 depletion through nitrogen fixation. An increase in NCP can in turn lead to O_2 depletion and the formation of H_2S in deeper water layers, due to the microbial oxidation of OM. Denitrification at the sedimentary or pelagic oxic/anoxic interface can promote N_2 production. The efficiencies of the latter processes in the Baltic Sea are favored by the years of stagnation in the deeper water layers of its central basins (Schneider et al., 2017).

The concentrations of gases dissolved in seawater is often determined based on the analysis of air at equilibrium with the seawater, a state reached using various equilibrators and with frequently direct contact between the gas and water phases. Measurements of discrete samples can be made using the conventional headspace method whereas bubble- or shower-type equilibrators or membrane equilibrators are used for continuous measurements. For an indirect estimate of the N_2 fixation, bubble-type equilibrators in combination with infrared spectroscopy have been used for continuous large scale surface-water pCO_2 (partial pressure of CO_2) records in the Baltic Sea (Schneider et al., 2009; Schneider et al., 2014a). The pCO_2 data were obtained using a fully automated measurement system deployed on a voluntary observing ship (VOS) traveling 4–5 times per week over a distance of > 1000 km across the entire central Baltic Sea. Changes in total CO_2 (C_T) were determined from the pCO_2 measurements. This method takes into account CO_2 gas exchange with the atmosphere and the formation of dissolved organic carbon to calculate seasonal C_T depletion, in turn facilitating estimates of the net production of particulate organic matter (POM) and thus NCP. The presence of NCP during mid-summer, when no DIN is available, implies the occurrence of N_2 fixation, which can be quantified on the basis of the mean C/N ratio of POM in mid-summer in the central Baltic Sea (Schneider et al., 2014a).

However, as this estimate of N_2 fixation is indirect, with many associated uncertainties, Schmale et al. (2019) developed an alternative approach in which a spray-type equilibrator is coupled with a mass spectrometer to obtain direct and continuous measurements of the N_2 concentration. The application of this method during a research cruise in mid-summer in the Baltic Sea revealed a distinct N_2 depletion in the surface water, attributed to N_2 fixation since it coincided with a clear draw-down of C_T in the absence of DIN. These findings demonstrated that mass spectrometry is sufficiently sensitive to detect the surface-water N_2 depletion caused by N_2 fixation. However, since the measurements were performed at different times in different regions, it was not possible to derive N_2 fixation rates.

Also, other established methods for quantifying N_2 fixation which are based on excess phosphorus consumption (PO_4 approach, Rahm et al., 2000), on the total nitrogen increase in surface water (TN approach, Larsson et al., 2001; Eggert et al., 2015), or on $^{15}N_2$ incubation (^{15}N approach, Montoya et al. 1996), have their limitations. The most significant shortcoming common to all three is related to their reliance on the analysis of discrete samples. Due to the patchiness of cyanobacterial blooms, measurements based on discrete samples can introduce significant uncertainties when extrapolating or interpolating the data in space and time. These shortcomings together with the interannual variability are reflected in the wide range of N_2 fixation estimates (310 - 792 kt-N/yr, Wasmund et al., 2005; Rolff et al., 2007) for the Baltic Proper. Still it indicates that the magnitude of the N_2 fixation is comparable to the combined waterborne (~250 kt/yr, HELCOM, 2023) and airborne (~105

kt/yr, HELCOM, 2023) inputs. To overcome the methodological limitations, high resolution continuous measurements are required, e.g. by the use of voluntary observing ships (VOS). These may provide continuous data with necessary temporal and spatial resolution along repeated fixed routes. Additionally, this approach captures transient N_2 fixation events more reliable than investigations during temporally limited research cruises.

A mass spectrometry technique for the analysis of gases dissolved in seawater was introduced in the early 1960s by Hoch and Kok (1963). The "membrane inlet mass spectrometry" (MIMS) uses a gas permeable membrane to separate a continuous flow of water from a gas phase (headspace), which has a direct connection to a mass spectrometer (MS). Due to the continuous pumping of the gas into the MS, low pressure in the gas side of the membrane equilibrator leads to a flow of the dissolved gases across the membrane into the gas side. As a result, a steady state is generated on the gas side of the equilibrator through the balance between the MS pumping rate (outflow) and the diffusion of the dissolved gases across the membrane (inflow). A requirement of this technique is the calibration of the system with seawater containing defined concentrations of the gases of interest. Due to the short response time MIMS facilitates the detection of fast changes in the dissolved gas concentrations, by reducing the ratio between the volume of the headspace and the gas flow into the MS. MIMS has been employed in the determination of NCP on the basis of the O_2/Ar ratio through which the physically shaped O_2 background concentration was separated from biogenic O_2 effects (Kaiser et al., 2005; Nemcek et al., 2008; Tortell et al., 2015).

The present study uses a modification of MIMS, the gas equilibrium-membrane-inlet mass spectrometry (GE-MIMS), which has been developed over the years through extensive work by different research groups. The most significant difference from MIMS is the establishment of a gas-phase equilibrium, which is maintained by the removal of only minor amounts of gas from the gas side of the membrane equilibrator. The mass spectrometric analysis of gases dissolved in water by the use of a membrane equilibrator was first suggested by Cassar et al. (2009) and Manning et al. (2016). Mächler et al. (2012) introduced the term "GE-MIMS" and made a first attempt for a semi-quantitative analysis of equilibrium partial pressures of dissolved gases, which were then related to the concentrations in the dissolved phase through the corresponding solubility constants. Since then, the GE-MIMS technique has been further refined for the quantitative determination of dissolved gas concentrations, as documented in various studies (Brennwald et al., 2016; Chatton et al, 2017, Weber et al., 2018) and Patent EP 4 109 092 A1 (Brennwald and Kipfer, 2022).

Our newly developed measurement system builds upon the established GE-MIMS approach, introducing a different calibration method and adapting it specifically for long term observations (e.g. on VOS) of the surface concentration of N_2 in order to detect and quantify N_2 fixation. The results will be supported by concurrent measurements of the O_2 concentration, which may provide complementary information about NCP, while determinations of the Ar concentration facilitate a reconstruction of abiotic conditions and allow for the determination of the gas exchange of N_2 and O_2.

The specific aims of this study were the following:

(1) determination of the completeness of the equilibration process and of the equilibration (response) time using commercially available membrane contactors;

(2) determination of the precision/accuracy of the gas analysis by mass spectrometry and estimates of the limits of detection for biogenic changes in N_2 concentrations;

(3) the prospective deployment of the GE-MIMS system on a VOS to better capture the importance of the N_2 fixation for the Baltic Sea nitrogen budget;

2 Measuring device

2.1 The membrane equilibrator

The principle of GE-MIMS is based on the establishment of an equilibrium between the partial pressures of a gas dissolved in water and in the gas phase. In the membrane equilibrator the water side and the gas side (comparable to a headspace) are separated by a gas-permeable membrane.

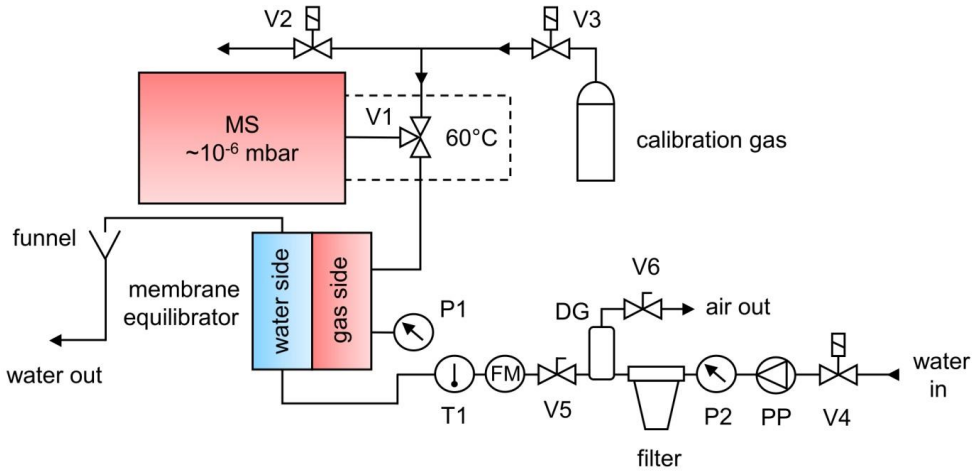

Figure 1: Schematic diagram of the gas equilibrium – membrane-inlet mass spectrometry (GE-MIMS) system. V1: 2-position valve (computer controlled), V2,3,4: solenoid valves (computer controlled), V5,6: valves, T1: temperature probe, P1,2: pressure sensors, PP: peristaltic pump, FM: flow meter, DG: degassing cylinder.

To ensure that the measurement system is appropriate for use at sea, it was tested in a laboratory setup designed as follows: A continuous flow of water is generated with the aid of a peristaltic pump. Seawater samples should be filtered prior to their contact with the membrane to prevent clogging of the pores through particles. This can be accomplished by installing a 10" polypropylene filter cartridge with a 5-µm pore size (sediment filter, Micro Rain Systems). A pressure gauge (P2) installed ahead of the filter indicates when the filter must be changed. For our setup, the filter cartridge had to be replaced at 1 bar overpressure to ensure system safety and reliability. Air trapped in the filter cartridge (particularly when the system is started) can be removed with the help of two valves (V5 and V6) and a degassing cylinder directly behind it. If laboratory experiments are conducted with distilled or tap water, filtration and the associated air removal are unnecessary.

The membrane equilibrator used in this study was the Liqui-Cel mini-module cartridge (1.8 × 8.75, model G541), containing porous hollow fibers made of gas-permeable hydrophobic polypropylene. The fibers are compactly arranged in a polycarbonate housing and provide a total membrane surface area of 0.9 m^2 exposed to a water volume of 70 mL. Due to the relatively large gas room (140 mL), the continuous flow of gas into the MS (6 µL/min) caused a pressure drop in the gas side of only 0.2 ‰ and thus had almost no effect for the establishment of the equilibration process (see Appendix A).

In addition to the Liqui-Cel membrane, we tested a membrane equilibrator produced by PermSelect (PDMSXA-1.0), in which the gas exchange between the water and gas phase is mediated by dense, non-porous hollow fibers consisting of polydimethylsiloxane (PDMS). Since the gas exchange does not take place across pores, clogging by particles that may hamper the gas flux is avoided by these membranes. However, testing with the PermSelect membrane revealed that it is unsuitable for our application. For reasons that remain unclear, water accumulates on the gas side of the membrane, which could potentially be sucked into the inlet of the MS and block gas flow into it. Furthermore, it affects vacuum stability and interferes with accurate mass spectrometric measurements.

Water temperature in the GE-MIMS system is measured by a temperature probe (T1, PT100, accuracy~~precision~~: 0.01°C) located at the inlet of the membrane. Total gas tension is recorded by connecting a pressure sensor (P1) (SEN 3276, Kobold, precision: 2 mbar) to the gas side of the membrane cartridge. A capillary connects the gas side of the equilibrator with the MS via V1.

A crucial aspect of the water flow system is to ensure that the water outlet is not positioned below the water level in the membrane equilibrator. Tests have shown that otherwise a suction effect occurs on the water side that reduces the total gas pressure in the equilibrator and thus disturbs the gas phase equilibrium.

Another aspect to be considered when using GE-MIMS for field studies is the effect of biofouling on membrane properties. Here, we suggest to regularly clean or even replace the membrane to maintain its performance. For field studies where there is a significant temperature difference between the water body under investigation and the laboratory, it is recommended to insulate the equilibrator to prevent the formation of water vapor condensate on the gas side of the membrane.

2.2 Mass spectrometry for N_2, Ar and O_2

A commercially available quadrupole mass spectrometer (QMS, GAM2000, InProcess Instruments) was used to analyze the gas composition on the gas side of the membrane equilibrator. A high vacuum (10^{-6} mbar) is generated within the MS through the combined use of a membrane pump and a turbomolecular pump. The sample gas is introduced to the ion source through a deactivated fused silica capillary (length: 3 m, internal diameter: 50 µm) connected to a 2-position valve (V1). To enhance MS signal stability, these parts are housed within a heated enclosure maintained at a constant temperature of 60 °C.

Using V1, either the gas side of the equilibrator or the calibration gas is connected to the MS by a capillary. It is crucial that the two capillaries have identical properties (length: 1.5 m, internal diameter: 50 µm) in order to maintain a constant internal pressure within the MS. The capillaries' dimensions limit the gas flow rate to approximately 6 µL/min according to the modified Hagen-Poiseuille equation (Cassar et al., 2009). This rate corresponds to a measured transfer time of approximately 80 s from the capillary inlet to detection.

During calibration, valve V3 connects the MS with the calibration gas, while valve V2 is opened to ambient air in order to prevent overpressure at V1. After calibration, V2 is closed in order to avoid contamination of the calibration line by ambient air through diffusion and to minimize its consumption.

Within the ion source of the MS, the sample molecules and atoms are ionized by electron impact ionization (70 eV). They are then separated in the quadrupole analyzer based on their mass-to-charge ratio (*m/z*) and ultimately detected and quantified using a Faraday cup. Alternatively, a secondary electron multiplier (SEM) can be used for both detection and quantification. However, systematic measurements (see below) have shown that for N_2 and O_2 the standard deviation is twice~~half~~ as large and the accuracy decreases when~~deviation from the target values is smaller~~ using the SEM~~Faraday cup~~ (Table 1), which may be due to its greater temperature sensitivity (Hoffmann et al., 2005; Khan et al., 2018).

For the quantification of N_2, O_2 and Ar, the respective ion currents can be extracted from the peaks of the nominal *m/z* ratios in the mass spectra (N_2: *m/z* = 28, O_2: *m/z* = 32, Ar: *m/z* = 40). During a 1-s measurement cycle, an ion current is detected for each gas species, which requires a measurement time of 340 ms per *m/z* ratio. Interferences with CO_2 fragments (CO^+, m/z = 28) can be ignored as discussed in Appendix B. For our laboratory tests, baseline correction was performed weekly using values at *m/z* = 3. However, baseline stability may vary depending on the location/platform, where the GE-MIMS is used. We recommend conducting additional tests during field operations to take field specific conditions.

We used a standard gas to calibrate the MS regularly (gas composition: $x(N_2)$: 78.1 %, $x(O_2)$: 20.9 %, x(Ar): 1.0 %), which we had previously recalibrated with clean, dry air. Calibration using such a standard gas is particularly important in areas where the standard composition of air is affected by exhaust gases, e.g. on a VOS. In environments where air pollution can be ruled out, the ambient air can also be used as the standard (e.g. Cassar et al., 2009; Mächler et al., 2012; Manning et al., 2016).We used Ar as an internal standard in order to reduce the effect of temperature or pressure fluctuations within the MS.

The calibration factors are given by the ratios I_X/I_{Ar} (ratio of the currents for gas X and Ar) divided by the ratios n_x/n_{Ar} (ratio between the molar amounts of X and Ar in the standard gas). From this calibration procedure it follows that elemental ratios

X/Ar for the analyzed gases (N_2/Ar, O_2/Ar and N_2/O_2) are the primary outcome of our MS measurements. The elemental ratios then yield mole fractions for N_2, O_2 and Ar with respect to the sum of N_2, O_2 and Ar. These mole fractions are called "incomplete" or in case that only water vapor effects the composition of the air "dry" mole fraction (calculations are presented in Appendix B).

Regarding the performance of the MS, it is important to take into account that the ionization process within the mass spectrometer is inherently pressure-dependent, resulting in variations in the ionization ratios of gases under different pressure conditions. To mitigate this, we effectively reduced the electron and ion density in the ion formation region by adjusting the emission current. This resulted in enhanced linearity in ion yield and fragmentation at different pressures. Indeed, our observations indicate that at pressures 200 mbar above the calibration conditions (atmospheric pressure), the relative change of the molar fraction of N_2 was 0.4 %. However, a total equilibrium pressure (total gas tension) of gases dissolved in surface seawater of more than 200 mbar above the atmospheric pressure, e.g., by biological or temperature effects, can be excluded. The performance of the GAM 2000-MS was evaluated by conducting 60 replicate measurements of ambient air over a period of 6 h, with ambient air calibration of the system being carried out between measurements throughout the entire period. The average of the 60 measurements was used to calculate the performance parameters of the MS (Table 1).

Table 1: Performance parameters of the GAM 2000-MS obtained by repeated measurements of the gases in ambient air. x_d : mole fraction deviation between the measured and the target value. *aSD*: absolute standard deviation, SEM: secondary electron multiplier.

Detector	Gas	x_d [$\times 10^{-3}$ %]	*aSD* [$\times 10^{-3}$ %]
Faraday cup	$^{28}N_2$	3.68	5.49
	$^{32}O_2$	3.44	5.31
	^{40}Ar	0.25	0.34
SEM	$^{28}N_2$	5.58	9.44
	$^{32}O_2$	5.41	9.06
	^{40}Ar	0.18	0.44

3 Performance of the concentration measurements

3.1 Accuracy and precision

The partial pressures of N_2, O_2 and Ar in the gas room of the membrane equilibrator (p_i) can be calculated by a modification of Dalton's Law (Eq. 1). Since incomplete mole fractions, which refer only to the total moles of the three considered gases (x_i', see the Appendix A), are used, the total pressure in the headspace (p_t) must be corrected for gases that were not measured, such as water vapor. However, the MS-based determination of water vapor is challenging due to the lack of a suitable calibration medium and the potential for overlapping *m/z* ratios, leading to imprecise measurements. Thus, water

vapor is instead determined by assuming saturation at the given temperature and salinity (Ambrose and Lawrenson, 1972). The contribution of other gases, e.g., CO_2, to the total pressure is assumed to be very minor and is neglected. The partial pressure of the considered gases is therefore calculated as shown in Eq. (1):

$$p_i = x_i' \cdot (p_t - pH_2O) \ , \quad (1)$$

Finally, the concentration of dissolved gases (c_i) in the water phase of the membrane equilibrator is calculated using the solubility constant, obtained from Hamme and Emerson (2004) for N_2 and Ar, and from Weiss (1970) for O_2, as shown in Eq. (2):

$$c_i = s_i \cdot p_i \ , \quad (2)$$

with:

s – solubility constant [mol · m^{-3} · atm^{-1}]

p – partial pressure

High instrument precision and accuracy are critical for measuring biogenic changes in N_2 and O_2 concentrations. This is particularly important in determinations of N_2 fixation in the Baltic Sea, as concentration deficits of only about 5 µmol-N_2/L (derived from the depth-integrated N_2 fixation in Schneider et al., 2014a) at a background concentration of about 500 µmol-N_2/L (at 20 °C) can be expected during moderate N_2 fixation activity in the central Baltic Sea.

The accuracy and precision of the concentration measurements were assessed by coupling the GE-MIMS with a temperature-controlled bath (Huber CC-K15) filled with distilled water. The thermostat was set to a constant temperature (T = 18.5 ± 0.02°C) and was open to the atmosphere in order to generate an equilibrium with atmospheric gases. The water was continuously recirculated through the membrane equilibrator at a flow rate of 2 L/min. Following calibration of the GE-MIMS, the mole fractions $x^{'}$ of N_2, O_2 and Ar and the total pressure of the gas phase were continuously measured for 1 h. After an initial adjustment period, the measured values were averaged (Δt ~ 20–60 min, Fig. 2) and used to determine the concentration (c_{meas}), the absolute and the relative standard deviation (*aSD* and *rSD*) of the concentrations of N_2, O_2 and Ar (Table 2).

The measured concentrations are presented together with the expected saturation concentrations (Hamme and Emerson, 2004; Weiss, 1970) in Fig. 2 and Table 2. The absolute standard deviation was very similar for N_2 and O_2, ranging from 0.15 µmol/L to 0.16 µmol/L. The measured concentration of Ar had a a*SD* that was an order of magnitude smaller. Additionally, the data indicated a 0.2 % offset for both N_2 and O_2 measurements. Due to the lower concentration values, the averaged offset was 0.7 % for Ar, twice as high as that of the other gases (Table 2).

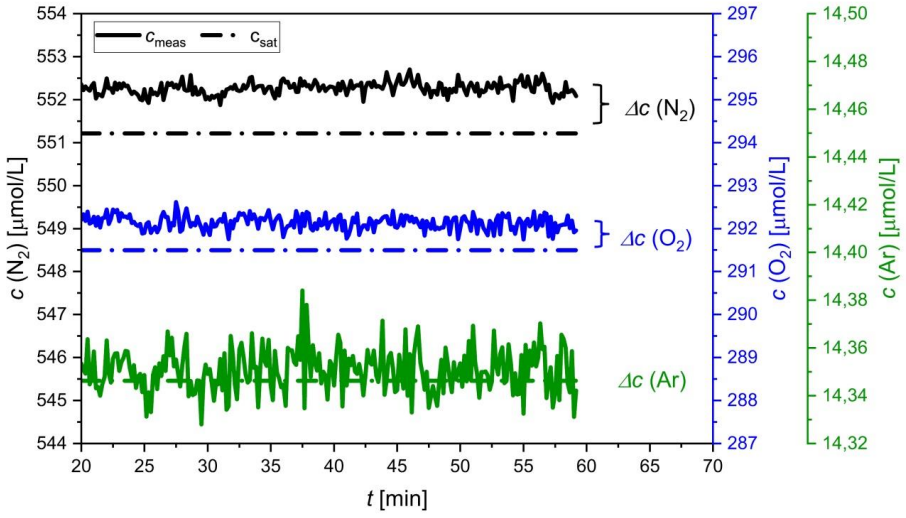

Figure 2: Concentration measurements of N_2 (black), O_2 (blue) and Ar (green) in distilled water equilibrated with ambient air during a laboratory experiment. While the measured values (c_{meas}) are indicated by solid lines, the saturation values (c_{sat}) are represented by the dotted lines.

The accuracy is given by the concentration difference (Δc) between the measured value (c_{meas}) and the saturation value (c_{sat}) of N_2, O_2 and Ar, as presented in Table 2. The precision is reported as the 2-fold absolute standard deviation (*aSD*).

Table 2: Results of a laboratory experiment in order to assess the accuracy and precision (2-fold *aSD*) of the GE-MIMS. *aSD*: absolute standard deviation, *rSD*: relative standard deviation.

Gas	*aSD* [µmol/L]	*rSD* [%]	Precision [µmol/L]	Precision [%]	c_{meas} [µmol/L]	c_{sat} [µmol/L]	Δc [µmol/L]	Δc [%]
$^{28}N_2$	0.15	0.03	0.30	0.05	552.3	551.2	1.1	0.2
$^{32}O_2$	0.16	0.05	0.32	0.11	292.1	291.5	0.6	0.2
^{40}Ar	0.01	0.07	0.02	0.14	14.4	14.3	0.1	0.7

The deviation of the measured N_2 concentration (Δc (N_2) = 1.1 µmol/L, Table 2) from the theoretical saturation values indicates that a moderately strong N_2 fixation episode of 5 µmol-N_2/L (derived from Schneider et al., 2014a), can be determined with an accuracy of about 20 %. This uncertainty refers also to the NCP associated with the N_2 fixation which at average conditions contributes by 20 – 26 % to the total annual NCP (Schneider and Müller, 2018).

3.2 Equilibration kinetics

3.2.1 Theory

The fundamental principle of a membrane equilibrator is that an equilibration process takes place between the partial pressures (p) of the water side (subscript "w") and the gas side (subscript "g") when they are separated by a gas permeable membrane. To derive a mathematical expression for the dependence~~y~~ of the equilibration time (τ) on the water flow rate (Q_w), we first consider the ~~case in which there is no water flow~~ continuous flow as a step-wise renewal of the water, where each time step corresponds to the mean residence time of the water in the equilibrator (water volume divided by water flow). It is then assumed that an equilibrium between the "stagnant" water and the gas phase is established during each time step. This is a plausible assumption in view of the dimensions of the membrane equilibrator (3M data sheet, 2021). The average thickness of the gas and water layer in the equilibrator is only 140 and 70 µm, respectively, and allows almost spontaneous equilibration. ~~The fundamental principle of a membrane equilibrator is that an equilibration process takes place between the partial pressures (p) of the water side (subscript "w") and the gas side (subscript "g") when they are separated by a gas permeable membrane.~~ However, interpretations of the equilibrium must take into account that gas exchange during the equilibration process affects both the gas phase and the dissolved phase. ~~The equilibrium p_g will therefore not be identical with the original p_w, as required by our approach to determine the gas concentration in the water. The increase/decrease in p_g during equilibration in relation to the original transmembrane partial pressure difference of a gas (Δp_0) can be derived as shown in~~ The partial pressure distribution after the first time step is given by Eq. (3), according to which, at equilibrium, the initial $p_{g,0}$ altered by Δp_g must be equal to the initial $p_{w,0}$ altered by Δp_w ($\Delta p_{w,g}$ refer to absolute changes):

$$p_{g,0} - \Delta p_g = p_{w,0} + \Delta p_w \,, \quad (3)$$

The initial Δp_0 can thus be expressed as shown in Eq. (4):

$$\Delta p_0 = \Delta p_g + \Delta p_w \,, \quad (4)$$

Δp_g and Δp_w can be expressed by the flux of moles (Δn) across the membrane, as shown in Eq. (5) and Eq. (6):

$$\Delta p_g = \frac{\Delta n \cdot R \cdot T}{V_g} \,, \quad (5)$$

$$\Delta p_w = \frac{\Delta n}{V_w \cdot s} \,, \quad (6)$$

with:

R – universal gas constant [$m^3 \cdot atm \cdot mol^{-1} \cdot K^{-1}$]

T – absolute temperature [K]

V – volume [m^3]

Combining Eq. (5) and Eq. (6) describes Δp_w as a function of Δp_g and yields Eq. (7):

$$\Delta p_w = \frac{\Delta p_g \cdot V_g}{V_w \cdot s \cdot R \cdot T} \,, \quad (7)$$

which together with Eq. (4) yields Eq. (8):

$$\Delta p_0 = \Delta p_g + \frac{\Delta p_g \cdot V_g}{V_w \cdot s \cdot R \cdot T}, \quad (8)$$

The ratio of Δp_g to the original Δp_0 is described by Eq. (9):

$$\frac{\Delta p_g}{\Delta p_0} = \frac{1}{1+\frac{V_g}{V_w \cdot s \cdot R \cdot T}}, \quad (9)$$

which shows that, after equilibration, the change in Δp_g in relation to the initial Δp_0 depends on the ratio of the gas and water volumes and on the solubility of the considered gas. For our Liqui-Cel membrane, the volume ratio V_w/V_g is 0.5 (3M data sheet, 2021) and results in a 0.8% change of Δp_g for N_2 with respect to the initial Δp_0 whereas, conversely, Δp_w changes by 99.2% of the initial Δp_0. This means that at equilibrium the partial pressure of the dissolved phase is close to that of the initial gas phase. However, our approach is based on a gas-phase partial pressure that is at equilibrium with water widely unaffected by gas exchange: $\Delta p_g/\Delta p_0 \approx 1$ or $\Delta p_w/\Delta p_0 \approx 0$. Even a 100-fold increase in the ratio to $V_w/V_g = 50$ would only yield a value of 0.45 for $\Delta p_g/\Delta p_0$. These calculations indicate that the water volume must approach infinity to achieve a 100% adjustment of $p_{g,0}$ to the initial $p_{w,0}$. The latter condition can be approximated by repeated renewal of the water through continuous pumping. ~~continuously pumping water through the water side of the equilibrator. The magnitude of the water flow thereby controls the kinetics of the equilibration process.~~

~~A central factor in this context is the equilibration time (τ), which is the time required for equilibrium to be established at a given partial pressure difference, thereby providing information on the temporal resolution of GE-MIMS measurements. For a flow-through system, a mathematical formulation of the equilibration time (τ) can be derived by considering time steps that correspond to the mean residence time, t_τ, of the water in the equilibrator. Therefore, it is assumed that during each time step t_τ an approximate equilibrium between the gas and the dissolved phase is repeatedly generated. This is a plausible assumption in view of the geometric dimensions of the membrane equilibrator, which imply that the thickness of the water and gas layers, given by the volumes of the water and gas side divided by the area of the membrane, amount to only 80 µm and 150 µm, respectively. As a consequence, the change in Δp_g after each renewal i is identical to the change in Δp_g according to Eq. (9).~~ Equation (9) was derived for the first time step, but it is of course valid for any time step (i) and the corresponding partial pressure difference Δp. Furthermore, the change in p_g may be interpreted as the reduction of the partial pressure difference after each water renewal. This may be approximated by a differential equation [Eq. (10)] using i as a variable:

$$\frac{d(\Delta p)}{di} = \frac{-1}{1+\frac{V_g}{V_w \cdot s \cdot R \cdot T}} \cdot (\Delta p)_i \ , \quad (10)$$

leading to Eq. (11):

$$d(\ln \Delta p) = \frac{-di}{1+\frac{V_g}{V_w \cdot s \cdot R \cdot T}}, \quad (11)$$

and integrating Eq. (11) yields Eq. (12):

Formatiert: Schriftart: Kursiv

Formatiert: Tiefgestellt

Formatiert: Schriftart: Kursiv

Formatiert: Tiefgestellt

$$\Delta p = \Delta p_0 \cdot \exp\left(\frac{-i}{1+\frac{V_g}{V_w \cdot s \cdot R \cdot T}}\right), \quad (12)$$

Since i is given by the elapsed time, t, divided by the residence time, t_r, Eq. (12) can be expressed by Eq. (13):

$$\Delta p = \Delta p_0 \cdot \exp\left[\frac{-t}{t_r \cdot \left(1+\frac{V_g}{V_w \cdot s \cdot R \cdot T}\right)}\right], \quad (13)$$

which describes the exponential development of the partial pressure difference towards equilibrium ($\Delta p = 0$).

And introducing the residence time at water flow conditions, τ:

$$\Delta p = \Delta p_0 \cdot \exp\left[\frac{-t}{\tau}\right], \quad (14)$$

where τ, is given as shown in Eq. (15):

$$\tau = t_r \cdot \left(1 + \frac{V_g}{V_w \cdot s \cdot R \cdot T}\right), \quad (15)$$

Equation (14) indicates that, after a time $t = \tau$, only $1/e$ of the original difference in the partial pressure remains. This implies that the equilibrium state has already reached approximately 63%. Consequently, after four times the equilibration time have elapsed, equilibrium has reached 99%.

Since the residence time is given by the water volume divided by the water flow rate, Q_w:

$$t_r = \frac{V_w}{Q_w}, \quad (16)$$

Eq. (17) is obtained:

$$\tau = \frac{V_w \cdot \left(1+\frac{V_g}{V_w \cdot s \cdot R \cdot T}\right)}{Q_w}, \quad (17)$$

An example is provided as follows: For the Liqui-Cel contactor used in our study and at a flow rate of 2 L/min, τ is 4.3 min for N_2, 2.2 min for O_2 and 2.0 min for Ar. The dependence of the equilibration time on water flow as well as on the solubility of the considered gas and the gas volume ~~different gases (different solubility constants) and V_g values~~ can be seen in Figure 3a, b, which depicts the hyperbolic-shaped functions described by Eq. (1~~2~~7); a significant increase in τ occurs at a water flow rate < 500 mL/min. The maximum flow of the membrane used in our study, according to the manufacturer's specification, is 3000 mL/min. Figure 3a shows that, due to the solubilities of O_2 and Ar, their τ are very similar, while τ of N_2 is about twice as long. A reduction in the gas volume of the membrane equilibrator leads to a corresponding decrease in τ (Figure 3b). ~~The maximum flow of the membrane used in our study, according to the manufacturer's specifications, is 3000 mL/min. All calculations in this section refer to a water temperature of 18 °C and a salinity of 7.~~

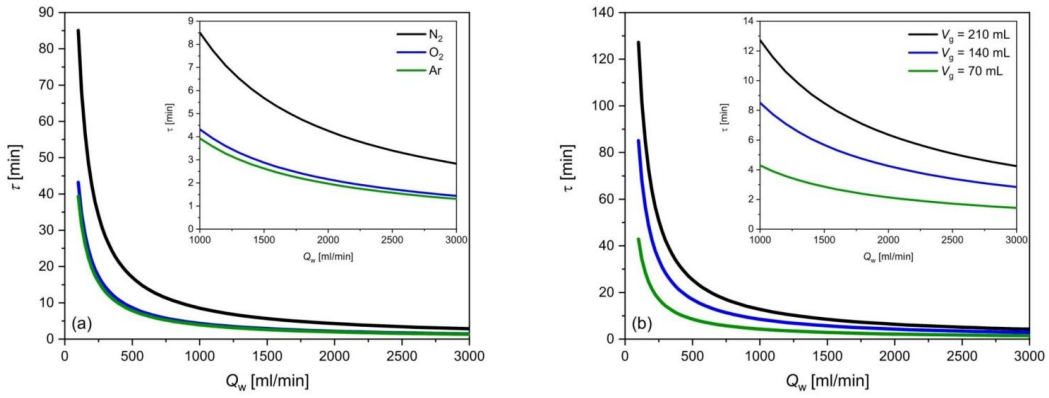

Figure 3: Theoretically determined dependence of the equilibration time τ on the water flow rate Q_w using the Liquicel 1.8x8.75 contactor (a) for different gas solubilities (N_2, O_2 and Ar) and (b) for N_2 and different gas side volumes of the membrane equilibrator (V_g of the Liquicel contactor: 140 mL). The insets show the typical flow-rate ranges at higher resolution.

The values for the different variables used in the previous calculations/Figures are as follows:

$R \cdot T = 2.39 \cdot 10^{-2}$ m^3 · atm · mol^{-1} (T = 18 °C)

$V_w = 0.7 \cdot 10^{-4}$ m^3 (3M data sheet, 2021)

$V_g = 1.4 \cdot 10^{-4}$ m^3 (3M data sheet, 2021)

$s(N_2) = 0.695$ mol · m^{-3} · atm^{-1} (Hamme and Emerson, 2004: T = 18 °C, Salinity = 7 PSU)

$s(Ar) = 1.519$ mol · m^{-3} · atm^{-1} (Hamme and Emerson, 2004: T = 18 °C, Salinity = 7 PSU)

$s(O_2) = 1.379$ mol · m^{-3} · atm^{-1} (Weiss, 1970: T = 18 °C, Salinity = 7 PSU)

Formatiert: Deutsch (Deutschland)

Formatiert: Englisch (USA)

Formatiert: Englisch (USA)

Formatiert: Englisch (USA)

Formatiert: Nicht Hochgestellt/ Tiefgestellt

Formatiert: Schriftart:

3.2.2 Measurement of τ

The equilibration time (τ) of the membrane equilibrator used in this study (Liqui-Cel 1.7 × 8.75) was also experimentally determined at flow-through conditions. For this purpose, 100-L containers were filled with tap water and allowed to rest for at least one day to allow for the development of a homogeneous water mass approximately at equilibrium with the atmosphere. A transmembrane partial pressure difference was generated by initially flushing the gas side of the membrane equilibrator with N_2. Subsequently, the water ($T \approx 18$°C) from the container was pumped through the water side at a flow rate of 2 L/min using the peristaltic pump. Adjustments of the N_2, O_2 and Ar partial pressures in the gas room to match those of these gases dissolved in water were recorded by MS determination of the mole fractions as well as measurement of the total pressure, as described in Sect. 3.1. Figure 4a shows an increase in the N_2 partial pressure after the gas side was flushed with N_2, followed by a decline due to equilibration with the partial pressure of N_2 dissolved in the water. The resulting plateau after approximately 30 min was considered to indicate equilibrium with atmospheric gases. The temporal evolution of the partial pressure difference on the gas side between the value at time t, $p_g(t)$, and the equilibrium value indicated by the

plateaued partial pressure at 30 min, p_g (eq), can be described by the exponential function shown in Eq. (18), which corresponds to Eq. (11):

$$p_g(t) - p_g(\text{eq}) = [p_g(t) - p_g(\text{eq})] \cdot e^{\left(\frac{-t}{\tau}\right)}, \quad (18)$$

Linearization of Eq. (18) yields an equation where ln [p_g (t) – p_g (eq)] is a linear function of t with a slope that corresponds to the reciprocal equilibration time, Eq. (19):

$$\ln[p_g(t) - p_g(\text{eq})] = -\frac{1}{\tau} \cdot t + \ln[p_g(t_0) - p_g(\text{eq})], \quad (19)$$

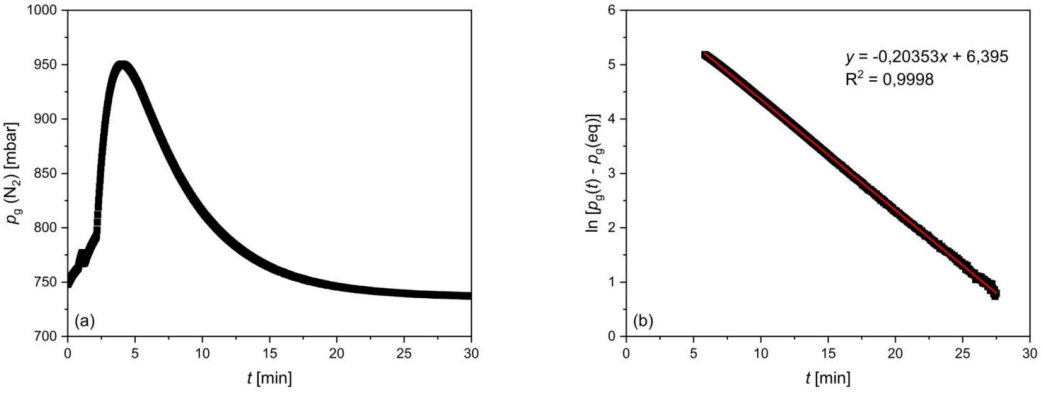

Figure 4: Results of an experiment to determine the equilibration time for N_2. (a) p_g (N_2) as a function of time. (b) The logarithmic presentation of the difference between the partial pressure of N_2 at any time t and after equilibrium is reached, as a function of time. The reciprocal slope of the regression line represents the *e*-fold equilibration time (τ).

The equilibration time τ was then determined from a regression line for ln [p_g (t) – p_g (eq)] as a function of t (Fig. 4b). The experiment described above was conducted three times, resulting in an average *e*-fold equilibration time ± *aSD* of τ (N_2) = 4.8 ± 0.1 min, τ (O_2) = 3.2 ± 0.1 min and τ (Ar) = 3.0 ± 0.2 min. These values differ from those determined theoretically using Eq. (17), but show the same order of magnitude. The deviations are attributed to the simplified assumptions inherent in the model. Critical points are that the model does not consider continuous water flow, but the transport of discrete water parcels through the equilibrator, and the assumption that a perfect equilibrium was generated repeatedly after each renewal (residence time) of the water in the membrane equilibrator.

The different equilibration times for the considered gases can be attributed to their different solubility constants, according to Eq. (17), with those of O_2 and Ar being similar and significantly below that of N_2. Compared with the τ (N_2/Ar) = 12 min achieved by coupling a MS to a spray-type equilibrator (Schmale et al., 2019), GE-MIMS is nearly three times faster.

Compared with other membrane equilibrator setups, where τ (Ar) = 4 min (Manning et al., 2016) or τ (O_2/Ar) = 7.75 min (Cassar et al., 2009), our system provides a slightly better temporal resolution.

If the GE-MIMS were installed on a VOS, then the spatial resolution (footprint) is given by the equilibration time and the ship's speed. Assuming an almost perfect equilibration after 4 τ and a typical ferry speed of about 20 kn, results in a spatial resolution of approximately 12 km for N_2, which is considered as the minimum scale for regional averaging of field data.

4 Quantification of biogeochemical process rates

The determination of biogeochemical process rates requires measurements of the respective variables as a function of time. The use of a VOS traveling across successive transects as a platform for GE-MIMS would enable the generation of a concentration time series over large areas such as the Baltic Proper (Schneider et al., 2007; Gülzow et al., 2011).

Any change in the N_2 concentration can be described as the effect of N_2 fixation and N_2 gas exchange with the atmosphere (Eq. 20) if vertical mixing across the thermocline is ignored. The latter is justified since N_2 fixation typically takes place during low wind speeds (< 5 m/s) which lead to a rising thermocline and warming of the surface layer (up to 22 °C) (Müller et al., 2021).

$$\Delta N_2 = \Delta N_{2,\mathrm{fix}} + \Delta N_{2,\mathrm{gas}}\,, \tag{20}$$

The concentration change due to gas exchange ($\Delta N_{2,\mathrm{gas}}$) during Δt (e.g., the time between two transects) within the mixed-layer depth, z_{mix}, is expressed by Eq. (21):

$$\Delta N_{2,\mathrm{gas}} = k_{660} \cdot \left(\frac{Sc_{N_2}}{660}\right)^{-0.5} \cdot (\bar{N}_{2,\mathrm{sat}} - \bar{N}_2) \cdot \frac{\Delta t}{z_{\mathrm{mix}}}\,, \tag{21}$$

where *Sc* is the Schmidt number (Wanninkhof, 1992) and $\bar{N}_{2,\mathrm{sat}}$ and $\bar{N}_2$ represent the values of the saturation concentration, averaged over a period of time (e.g., between two consecutive transects) and calculated based on the respective averaged temperature and salinity, and of the measured concentration, respectively. The transfer velocity of gas exchange (k_{660}) varies with wind speed and can be estimated using parameterizations such as that suggested by Wanninkhof et al. (2009). However, especially at low wind speeds and during periods of increased OM production, this method is subject to considerable uncertainties. For example, the presence of organic surface films can significantly reduce gas exchange, a phenomenon that current transfer velocity parameterizations do not adequately address. Therefore, concurrent Ar measurements are included to circumvent the uncertainties in using parameterizations of the transfer velocity. This approach is based on the observation that N_2 fixation events usually coincide with a significant increase in surface temperature (Schneider et al., 2014b; Schmale et al., 2019), such that the partial pressure of Ar in the surface water increases, which in turn leads to an Ar flux into the atmosphere. The change in the Ar concentration due to gas exchange at the water surface can be calculated using Eq. (22), which is similar to Eq. (21):

$$\Delta Ar_{\mathrm{gas}} = k_{660} \cdot \left(\frac{Sc_{Ar}}{660}\right)^{-0.5} \cdot (\bar{A}r_{\mathrm{sat}} - \bar{A}r) \cdot \frac{\Delta t}{z_{\mathrm{mix}}}\,, \tag{22}$$

Nitrogen gas exchange can then be quantified without explicitly calculating k_{660}, since combining Eq. (21) and (22) yields Eq. (23):

$$\Delta N_{2,gas} = \Delta Ar \cdot \left(\frac{Sc_{N2}}{Sc_{Ar}}\right)^{-0.5} \cdot \frac{\bar{N}_{2,sat} - \bar{N}_2}{\bar{A}r_{sat} - \bar{A}r}, \quad (23)$$

Finally, the difference in the nitrogen concentration due to N_2 fixation for a certain time interval can be obtained using Eq. (24):

$$\Delta N_{2,fix} = \Delta N_2 - \Delta Ar \cdot \left(\frac{Sc_{N2}}{Sc_{Ar}}\right)^{-0.5} \cdot \frac{\bar{N}_{2,sat} - \bar{N}_2}{\bar{A}r_{sat} - \bar{A}r}, \quad (24)$$

Because of the low wind speed and the surface accumulation of OM during a cyanobacterial bloom, it is assumed that gas exchange is of minor importance and that the temporal change in the measured nitrogen concentration ΔN_2 is the main term (Wasmund, 1997; Lips and Lips, 2008; Schmale et al., 2019).

Eq. (24) includes implicitly the calculation of k_{660} which can be determined explicitly from the Ar measurement by the use of Eq. (22):

$$k_{660} = \frac{\Delta Ar \cdot z_{mix}}{(Sc_{Ar}/660)^{-0.5} \cdot (\bar{A}r_{sat} - \bar{A}r) \cdot \Delta t}, \quad (24)$$

Therefore, continuous measurements with our newly developed GE-MIMS system can also be used to determine k_{660}, provided the mixed-layer depth (z_{mix}) can be estimated, e.g., by modelling the surface water temperature and salinity profiles (Gräwe et al., 2019).

5 Conclusion

The results from our laboratory tests demonstrated that the GE-MIMS system is capable of directly determining cyanobacterial N_2 consumption and potentially also the associated O_2 production resulting from photosynthesis triggered by N_2 fixation. Ar concentrations for both the parametrization of air-sea gas exchange and for the reconstruction of abiotic background concentrations of biogeochemically active gases such as N_2 and O_2 could be measured with high precision and accuracy. Our measurement system is based on the same principle as that of Schmale et al. (2019), but it uses a membrane equilibrator, which in contrast to bubble/shower-type equilibrators, do not require ventilation and therefore constitutes a closed system. This ensures that the partial pressures in the gas phase are truly at equilibrium with the dissolved gases rather than merely at steady state (Schneider et al., 2007),

The individual components are designed to allow autonomous long term operation of the measurement system, particularly when installed on a VOS, such as that currently used for continuous pCO_2 measurements in the Baltic Sea (Gülzow et al., 2011; Schneider et al., 2014b; Jacobs et al. 2021). The resulting N_2, O_2 and Ar concentration time series will facilitate determinations of N_2 fixation rates and potentially NCP in selected regions of the Baltic Sea. The temporal dynamics of the above-mentioned biogeochemical processes can also be investigated. Furthermore, synchronous measurements of surface N_2(Ar) and pCO_2, take advantage of both the direct determination of N_2 consumption by fixation and the high sensitivity of

the CO_2 approach to production events (Schneider and Müller, 2018). The main limitations of existing approaches to quantifying N_2 fixation, which result from the analysis of discrete samples and the use of the elemental composition of POM, are thus circumvented. Furthermore, the possibility of averaging over larger spatial scales due to the operation of the GE-MIMS on a VOS enhances its compatibility with process-based model results, which typically have a spatial resolution of several kilometers.

Appendix A: Pressure effect of the gas flow into the mass spectrometer

To estimate the effect of the continuous flow of gas into the MS (6 µL/min) on the pressure in the gas room (p_g), the development of a steady state in the gas room is considered. The latter is based on a balance between the gas flow into the MS (F_{MS}) and the flux of dissolved gases into the gas room (F_g) which are given by Eq. (25) and Eq. (26):

$$F_{MS} = Q_V \cdot \frac{p_g}{R \cdot T}, \text{ [mol} \cdot \text{s}^{-1}\text{]} \quad (25)$$

$$F_g = k_n \cdot A \cdot (p_{atm} - p_g), \text{ [mol} \cdot \text{s}^{-1}\text{]} \quad (26)$$

with:

Q_v - volume flow into the MS: $1 \cdot 10^{-10}$ $m^3 \cdot s^{-1}$

k_n – transfer coefficient: $2.21 \cdot 10^{-5}$ mol $\cdot$ $s^{-1} \cdot m^{-2} \cdot atm^{-1}$ (derived from the experimentally determined equilibration time, see Appendix C~~D~~)

A – membrane area: 0.92 m^2

$R \cdot T = 2.39 \cdot 10^{-2}$ $m^3 \cdot atm \cdot mol^{-1}$ (T = 18 °C)

p_g – pressure in the gas room [atm]

p_{atm} – total pressure of the dissolved gases, approximately 1 atm

Equation (25) and Eq. (26) lead to the mass balance described in Eq. (27) for the steady state:

$$Q_V \cdot \frac{p_g}{R \cdot T} = k_n \cdot A \cdot (p_{atm} - p_g), \quad (27)$$

Rearranging Eq. (27) yields an expression that describes the effect of the gas flow into the MS through the ratio between pressure in the gas room (p_g) and "true" equilibrium pressure (p_{atm}) that was assumed to be 1 atm, as shown in Eq. (28):

$$\frac{p_g}{p_{atm}} = \frac{1}{1 + \frac{Q_V}{R \cdot T \cdot k_n \cdot A}}, \quad (28)$$

Using the values for the variables in Eq. (28) as given above, results in a ratio p_g/p_{atm} = 0.9998 which means that the pressure in the gas room deviated by 0.2 ‰ from the equilibrium total pressure.

Formatiert: Englisch (USA)

Appendix B: Evaluation of mass spectrometric data

In the initial step, ion currents corresponding to the specific mass-to-charge ratios of the following gases are measured using the mass spectrometer: N_2; *m/z* = 28, O_2; *m/z* = 32, and Ar; *m/z* = 40. We are aware that the *m/z* ratio for nitrogen may include interferences with other fragment ions, such as from carbon dioxide (CO^+). However, based on the manuscript of Burlacot et al. (2020), only 9.81 % of the primary CO_2 signal at *m/z* = 44 is fragmented into the CO ion at *m/z* = 28. Assuming CO_2 concentration close to atmospheric equilibrium concentrations, this would correspond to around 40 ppm of CO, which interfere with the N_2 quantification (at atmospheric N_2 concentrations of 78 %). This level of interference is negligible. Furthermore, regarding envisaged measurements on a VOS in the Baltic Sea, the risk of interference becomes even lower because CO_2 in the surface waters of the Baltic Sea is strongly undersaturated with respect to atmospheric CO_2 during periods of N_2 fixation due to concurrent biological production (Schneider et al., 2007).

For calibration a gas mixture characterized by precisely defined molar ratios (*n*/*n*) of N_2, O_2 and Ar is used to transform the ion currents (*I*) into mole fractions (*x*). Therefore, calibration factors are determined which are based on the ion currents of N_2 and O_2 normalized to the ion current of Ar as internal standard. The calibration factors are then obtained by relating the normalized ion currents to the corresponding molar ratio between the considered gas and Ar, as shown in Eq. (29) and Eq. (40):

$$F_{\mathrm{cal,N2}} = \frac{\frac{I_{\mathrm{N2}}}{I_{\mathrm{Ar}}}}{\frac{n_{\mathrm{N2}}}{n_{\mathrm{ArN2}}}}\,, \tag{29}$$

$$F_{\mathrm{cal,O2}} = \frac{\frac{I_{\mathrm{O2}}}{I_{\mathrm{Ar}}}}{\frac{n_{\mathrm{O2}}}{n_{\mathrm{Ar}}}}\,, \tag{30}$$

Once the calibration factors are determined, measurements of the ion currents for N_2, O_2 and Ar yield the molar ratios n_{O2}/n_{Ar}, n_{N2}/n_{Ar} and, consequently, n_{O2}/n_{N2}. These can be used to calculate the mole fractions (x') of N_2, O_2 and Ar with respect to the sum of N_2, O_2 and Ar, resulting in Eq. (31) to Eq. (33):

$$\frac{n_{\mathrm{O2}}}{n_{\mathrm{Ar}}} + \frac{n_{\mathrm{N2}}}{n_{\mathrm{Ar}}} + 1 = \frac{1}{x'_{\mathrm{Ar}}}\,, \tag{31}$$

$$\frac{n_{\mathrm{O2}}}{n_{\mathrm{N2}}} + \frac{n_{\mathrm{Ar}}}{n_{\mathrm{N2}}} + 1 = \frac{1}{x'_{\mathrm{N2}}}\,, \tag{32}$$

$$\frac{n_{\mathrm{N2}}}{n_{\mathrm{O2}}} + \frac{n_{\mathrm{Ar}}}{n_{\mathrm{O2}}} + 1 = \frac{1}{x'_{\mathrm{O2}}}\,, \tag{33}$$

Since the analyzed gas, e.g. ambient air, may contain other gases than N_2, O_2 and Ar, x' is considered as the incomplete mole fraction. In case that only water vapor is taken into account, the incomplete mole fraction is also called “dry” mole fraction. Consequently, x' of N_2, O_2 and Ar must to be multiplied with the “incomplete” total pressure in order to calculate the corresponding partial pressures. In analogy to the incomplete mole fraction, the “incomplete” is given by the total pressure (p_t) minus the partial pressures of gases (p_x) such as water vapor, that were not included in the definition of the partial mole fraction, x', e.g. as shown for the partial pressure of N_2 in Eq. (34):

$$p_{\mathrm{N2}} = x'_{\mathrm{N2}} \cdot (p_{\mathrm{t}} - p_{\mathrm{H2O}} - \sum p_{\mathrm{x}})\,, \tag{34}$$

Appendix C: Calculation of the transfer coefficient, k_n

To calculate the transfer coefficient, k_n, we first derive an equation for the equilibration time, τ_{nf}, for the hypothetical case in which there is no water flow (see Sec. 3.2.1). The flux across the membrane is driven by the partial pressure difference according to the general flux equation [Eq. (35)]:

$$\frac{\partial n_g}{\partial t \cdot A} = -k_n \cdot \Delta p \,, \tag{35}$$

with:

$\frac{\partial n}{\partial t}$ – change with time of the moles of a gas in the gas side of the equilibrator [mole · s^{-1}]

A – membrane area [m^2]

k_n – mass (mole) transfer coefficient~~nstant~~ [mol · s^{-1} · m^{-2} · atm^{-1}]

Δp – partial pressure difference: p_g - p_w [atm]

subscript g refers to the gas side of the membrane equilibrator and w to the water side

Using the ideal gas law, ∂n_g is replaced by ∂p_g according to Eq. (36):

$$\frac{\partial p_g}{\partial t} = \frac{-k_n \cdot A \cdot R \cdot T}{V_g} \cdot \Delta p \,, \tag{36}$$

with:

∂p - change in the partial pressure of a gas [atm]

R – universal gas constant [m^3 · atm · mol^{-1} · K^{-1}]

T – absolute Temperature [K]

V – volume [m^3]

To describe Δp only as a function of p_g, the total moles (gas side + water side) of the considered gas, n_t, which is constant at zero flow, is introduced, as shown in Eq. (37):

$$n_t = V_g \cdot \frac{p_g}{R \cdot T} + V_w \cdot p_w \cdot s \,, \tag{37}$$

with:

s – solubility constant [mol · m^{-3} · atm^{-1}]

p_w is thus given as shown in Eq. (38):

$$p_w = \frac{n_t - \left(\frac{p_g}{R \cdot T}\right) \cdot V_g}{V_w \cdot s} \,, \tag{38}$$

and Δp is expressed using Eq. (39):

$$\Delta p = p_g - \frac{n_t - \left(\frac{p_g}{R \cdot T}\right) \cdot V_g}{V_w \cdot s} \,, \tag{39}$$

The differentiation of Eq. (39) yields Eq. (40):

$$d(\Delta p) = \left(1 + \frac{V_g}{R \cdot T \cdot V_w \cdot s}\right) dp_g \,, \tag{40}$$

Replacing ∂p_g in Eq. (36) then yields Eq. (41):

$$\frac{d(\Delta p)}{dt} = -k_n \cdot A \cdot \left(\frac{R \cdot T}{V_g} + \frac{1}{s \cdot V_w}\right) \cdot \Delta p \,, \tag{41}$$

The integration of which provides an exponential equation [Eq. (42)]:

$$\Delta p = \Delta p_0 \cdot \exp\left[-k_n \cdot A \cdot \left(\frac{R \cdot T}{V_g} + \frac{1}{s \cdot V_w}\right) \cdot t\right], \tag{42}$$

with a time constant [s^{-1}] that equals the reciprocal equilibration time $\frac{1}{\tau_{nf}}$ (no water flow), resulting in Eq. (43) and Eq. (44):

$$\Delta p = \Delta p_0 \cdot \exp\left(\frac{-t}{\tau_{nf}}\right), \tag{43}$$

$$\tau_{nf} = \frac{1}{k_n \cdot A \cdot \left(\frac{R \cdot T}{V_g} + \frac{1}{V_w \cdot s}\right)}, \tag{44}$$

In addition to the geometric dimensions (V_g = 1.40 · 10^{-46} m^3, A = 0.92 m^2) of the membrane equilibrator and the thermodynamic properties, the gas exchange and thus the equilibration time is controlled by the transfer coefficient k_n. The latter can be calculated, using the experimentally determined equilibration times (τ (N_2) = 288 s, Sec. 3.2.2). Since these were determined with a water flow, we assume that V_w is infinitely large, thereby modifying Eq. (44) to yield Eq. (45) and thus k_n for N_2:

$$k_n = \frac{V_g}{\tau \cdot A \cdot R \cdot T}, \tag{45}$$

k_n = 2.21 · 10^{-5} mol · m^{-2} · s^{-1} · atm^{-1}.

Data availability

The data used to reproduce the results presented here are archived at http://doi.io-warnemuende.de/10.12754/data-2024-0014 (Iwe, 2024).

Author contribution

All the authors developed the idea and the design of this manuscript, and SI performed the laboratory experiments. The theoretical considerations of the equilibration process based on the equations were mainly carried out by BS. The paper was mainly written by SI, with major comments and revisions by OS and BS. All the authors contributed to the article and approved the submitted version.

Competing interests

The authors declare that they have no conflict of interest.

Acknowledgments

We thank Bernd Sadkowiak for his assistance in the construction of the measurement setup, Stefan Otto and Michael Glockzin for supporting the laboratory experiments and Sebastian Neubert for programming a data logger (all at IOW).

Financial support

This study received funding from the German Research Foundation (SCHM 2530/8-1, SCHN582/9-1).

References

3M data sheet, 3M™ Liqui-Cel™ MM-1.7x8.75 Series Membrane Contactor, Rev. 02: https://multimedia.3m.com/mws/media/1412495O/3m-liqui-cel-mm-1-7x8-75-series-membrane-contactor.pdf, last access: 24.10.2024, 2021.

Ambrose, D. and Lawrenson, I. J.: The vapour pressure of water, J. Chem. Thermodyn., 4, 755–761, https://doi.org/10.1016/0021-9614(72)90049-3, 1972.

Benson, B. B. and Parker, P. D. M.: Nitrogen/argon and nitrogen isotope ratios in aerobic sea water, Deep Sea Res. 1953, 7, 237–253, https://doi.org/10.1016/0146-6313(61)90042-9, 1961.

Brennwald, M. S., Schmidt, M., Oser, J., and Kipfer, R.: A Portable and Autonomous Mass Spectrometric System for On-Site Environmental Gas Analysis, Environ. Sci. Technol., 50, 13455–13463, https://doi.org/10.1021/acs.est.6b03669, 2016.

Brennwald, M. S. and Kipfer, R., 2022: Gas-equilibrium membrane inlet mass spectrometry with accurate quantification of dissolved-gas partial pressures (GE-MIMS-APP). Patent EP 4 109 092 A1, European Patent Office.

Burlacot, A., Burlacot, F., Li-Beisson, Y., and Peltier, G.: Membrane Inlet Mass Spectrometry: A Powerful Tool for Algal Research, Front. Plant Sci., 11, https://doi.org/10.3389/fpls.2020.01302, 2020.

Cassar, N., Barnett, B. A., Bender, M. L., Kaiser, J., Hamme, R. C., and Tilbrook, B.: Continuous High-Frequency Dissolved O_2/Ar Measurements by Equilibrator Inlet Mass Spectrometry, Anal. Chem., 81, 1855–1864, https://doi.org/10.1021/ac802300u, 2009.

Chatton, E., Labasque, T., de La Bernardie, J., Guihéneuf, N., Bour, O., and Aquilina, L.: Field Continuous Measurement of Dissolved Gases with a CF-MIMS: Applications to the Physics and Biogeochemistry of Groundwater Flow, Environ. Sci. Technol., 51, 846–854, https://doi.org/10.1021/acs.est.6b03706, 2017.

Craig, H. and Hayward, T.: Oxygen Supersaturation in the Ocean: Biological Versus Physical Contributions, Science, 235, 199–202, https://doi.org/10.1126/science.235.4785.199, 1987.

Eggert, A. and Schneider, B.: A nitrogen source in spring in the surface mixed-layer of the Baltic Sea: Evidence from total nitrogen and total phosphorus data, J. Mar. Syst., 148, 39–47, https://doi.org/10.1016/j.jmarsys.2015.01.005, 2015.

Gräwe, U., Klingbeil, K., Kelln, J., and Dangendorf, S.: Decomposing Mean Sea Level Rise in a Semi-Enclosed Basin, the Baltic Sea, J. Clim., 32, 3089–3108, https://doi.org/10.1175/JCLI-D-18-0174.1, 2019.

Gülzow, W., Rehder, G., Schneider, B., Deimling, J. S. v., and Sadkowiak, B.: A new method for continuous measurement of methane and carbon dioxide in surface waters using off-axis integrated cavity output spectroscopy (ICOS): An example from the Baltic Sea, Limnol. Oceanogr. Methods, 9, 176–184, https://doi.org/10.4319/lom.2011.9.176, 2011.

Hamme, R. C. and Emerson, S. R.: The solubility of neon, nitrogen and argon in distilled water and seawater, Deep Sea Res. Part Oceanogr. Res. Pap., 51, 1517–1528, https://doi.org/10.1016/j.dsr.2004.06.009, 2004.

HELCOM (2023) Inputs of nutrients to the sub-basins (2021). HELCOM core indicator report: https://indicators.helcom.fi/indicator/inputs-of-nutrients/, last access: 18.10.2024, ISSN 2343-2543.

Hoch, G. and Kok, B.: A mass spectrometer inlet system for sampling gases dissolved in liquid phases, Arch. Biochem. Biophys., 101, 160–170, https://doi.org/10.1016/0003-9861(63)90546-0, 1963.

Hoffmann, D. L., Richards, D. A., Elliott, T. R., Smart, P. L., Coath, C. D., and Hawkesworth, C. J.: Characterisation of secondary electron multiplier nonlinearity using MC-ICPMS, Int. J. Mass Spectrom., 244, 97–108, https://doi.org/10.1016/j.ijms.2005.05.003, 2005.

Iwe, S.: Characterizing the Gas Equilibrium - Membrane-Inlet Mass Spectrometer (GE-MIMS) through Laboratory Data, IOW [dataset], http://doi.io-warnemuende.de/10.12754/data-2024-0014, 2024.

Jacobs, E., Bittig, H. C., Gräwe, U., Graves, C. A., Glockzin, M., Müller, J. D., Schneider, B., and Rehder, G.: Upwelling-induced trace gas dynamics in the Baltic Sea inferred from 8 years of autonomous measurements on a ship of opportunity, Biogeosciences, 18, 2679–2709, https://doi.org/10.5194/bg-18-2679-2021, 2021.

Jahangir, M. M. R., Johnston, P., Khalil, M. I., Grant, J., Somers, C., and Richards, K. G.: Evaluation of headspace equilibration methods for quantifying greenhouse gases in groundwater, J. Environ. Manage., 111, 208–212, https://doi.org/10.1016/j.jenvman.2012.06.033, 2012.

Kaiser, J., Reuer, M. K., Barnett, B., and Bender, M. L.: Marine productivity estimates from continuous O2/Ar ratio measurements by membrane inlet mass spectrometry, Geophys. Res. Lett., 32, https://doi.org/10.1029/2005GL023459, 2005.

Khan, M. I., Lubner, S. D., Ogletree, D. F., and Dames, C.: Temperature dependence of secondary electron emission: A new route to nanoscale temperature measurement using scanning electron microscopy, J. Appl. Phys., 124, 195104, https://doi.org/10.1063/1.5050250, 2018.

Larsson, U., Hajdu, S., Walve, J., and Elmgren, R.: Baltic Sea nitrogen fixation estimated from the summer increase in upper mixed layer total nitrogen, Limnol. Oceanogr., 46, 811–820, https://doi.org/10.4319/lo.2001.46.4.0811, 2001.

Formatiert: Standard

Formatiert: Standard

Lips, I. and Lips, U.: Abiotic factors influencing cyanobacterial bloom development in the Gulf of Finland (Baltic Sea), Hydrobiologia, 614, 133–140, https://doi.org/10.1007/s10750-008-9449-2, 2008.

Mächler, L., Brennwald, M. S., and Kipfer, R.: Membrane Inlet Mass Spectrometer for the Quasi-Continuous On-Site Analysis of Dissolved Gases in Groundwater, Environ. Sci. Technol., 46, 8288–8296, https://doi.org/10.1021/es3004409, 2012.

Manning, C. C., Stanley, R. H. R., and Lott, D. E. I.: Continuous Measurements of Dissolved Ne, Ar, Kr, and Xe Ratios with a Field-Deployable Gas Equilibration Mass Spectrometer, Anal. Chem., 88, 3040–3048, https://doi.org/10.1021/acs.analchem.5b03102, 2016.

Montoya, J. P., Voss, M., Kahler, P., and Capone, D. G.: A Simple, High-Precision, High-Sensitivity Tracer Assay for N(inf2) Fixation, Appl. Environ. Microbiol., 62, 986–993, 1996.

Müller, J. D., Schneider, B., Gräwe, U., Fietzek, P., Wallin, M. B., Rutgersson, A., Wasmund, N., Krüger, S., and Rehder, G.: Cyanobacteria net community production in the Baltic Sea as inferred from profiling pCO_2 measurements, Biogeosciences, 18, 4889–4917, https://doi.org/10.5194/bg-18-4889-2021, 2021.

Nemcek, N., Ianson, D., and Tortell, P. D.: A high-resolution survey of DMS, CO_2, and O_2/Ar distributions in productive coastal waters, Glob. Biogeochem. Cycles, 22, https://doi.org/10.1029/2006GB002879, 2008.

Rahm, L., Jönsson, A., and Wulff, F.: Nitrogen fixation in the Baltic proper : An empirical study, J. Mar. Syst., 25, 239–248, 2000.

Redfield, A. C., Ketchum, B. H., and Richards, F. A.: The influence of organisms on the composition of sea-water, in: The sea: ideas and observations on progress in the study of the seas, edited by: Hill, M. N., Interscience, New York, 26-77, ISBN: 9780674017283, 1963.

Rolff, C., Almesjö, L., and Elmgren, R.: Nitrogen fixation and abundance of the diazotrophic cyanobacterium Aphanizomenon sp. in the Baltic Proper, Mar. Ecol.-Prog. Ser. - MAR ECOL-PROGR SER, 332, 107–118, https://doi.org/10.3354/meps332107, 2007.

Schmale, O., Karle, M., Glockzin, M., and Schneider, B.: Potential of Nitrogen/Argon Analysis in Surface Waters in the Examination of Areal Nitrogen Deficits Caused by Nitrogen Fixation, Environ. Sci. Technol., 53, 6869–6876, https://doi.org/10.1021/acs.est.8b06665, 2019.

Schneider, B., Sadkowiak, B., and Wachholz, F.: A new method for continuous measurements of O_2 in surface water in combination with pCO_2 measurements: Implications for gas phase equilibration, Mar. Chem., 103, 163–171, https://doi.org/10.1016/j.marchem.2006.07.002, 2007.

Schneider, B., Kaitala, S., Raateoja, M., and Sadkowiak, B.: A nitrogen fixation estimate for the Baltic Sea based on continuous pCO_2 measurements on a cargo ship and total nitrogen data, Cont. Shelf Res., 29, 1535–1540, https://doi.org/10.1016/j.csr.2009.04.001, 2009.

Schneider, B., Gustafsson, E., and Sadkowiak, B.: Control of the mid-summer net community production and nitrogen fixation in the central Baltic Sea: An approach based on pCO_2 measurements on a cargo ship, J. Mar. Syst., 136, 1–9, https://doi.org/10.1016/j.jmarsys.2014.03.007, 2014a.

Schneider, B., Gülzow, W., Sadkowiak, B., and Rehder, G.: Detecting sinks and sources of CO2 and CH4 by ferrybox-based measurements in the Baltic Sea: Three case studies, J. Mar. Syst., 140, 13–25, https://doi.org/10.1016/j.jmarsys.2014.03.014, 2014b.

Schneider, B., Dellwig, O., Kuliński, K., Omstedt, A., Pollehne, F., Rehder, G., and Savchuk, O.: Biogeochemical cycles, in: Biological Oceanography of the Baltic Sea, edited by: Snoeijs-Leijonmalm, P., Schubert, H., and Radziejewska, T., Springer, Dordrecht, Netherlands, 87-122, https://doi.org/10.1007/978-94-007-0668-2_3, 2017.

Schneider, B. and Müller, J. D.: Biogeochemical Transformations in the Baltic Sea: Observations Through Carbon Dioxide Glasses, 1st ed., Springer Oceanography, Springer International Publishing AG, Cham, 110 pp., https://doi.org/10.1007/978-3-319-61699-5, 2018.

Tortell, P. D., Bittig, H. C., Körtzinger, A., Jones, E. M., and Hoppema, M.: Biological and physical controls on N_2, O_2, and CO_2 distributions in contrasting Southern Ocean surface waters, Glob. Biogeochem. Cycles, 29, 994–1013, https://doi.org/10.1002/2014GB004975, 2015.

Wanninkhof, R.: Relationship between wind speed and gas exchange over the ocean, J. Geophys. Res. Oceans, 97, 7373–7382, https://doi.org/10.1029/92JC00188, 1992.

Wanninkhof, R., Asher, W. E., Ho, D. T., Sweeney, C., and McGillis, W. R.: Advances in Quantifying Air-Sea Gas Exchange and Environmental Forcing*, Annu. Rev. Mar. Sci., 1, 213–244, https://doi.org/10.1146/annurev.marine.010908.163742, 2009.

Wasmund, N.: Occurrence of cyanobacterial blooms in the baltic sea in relation to environmental conditions, Int. Rev. Gesamten Hydrobiol. Hydrogr., 82, 169–184, https://doi.org/10.1002/iroh.19970820205, 1997.

Wasmund, N., Nausch, G., Schneider, B., Nagel, K., and Voss, M.: Comparison of nitrogen fixation rates determined with different methods: a study in the Baltic Proper, Mar. Ecol. Prog. Ser., 297, 23–31, https://doi.org/10.3354/meps297023, 2005.

Weber, U. W., Cook, P. G., Brennwald, M. S., Kipfer, R., and Stieglitz, T. C.: A Novel Approach To Quantify Air–Water Gas Exchange in Shallow Surface Waters Using HighResolution Time Series of Dissolved Atmospheric Gases, Environ. Sci. Technol., 53, 1463– 1470, https://doi.org/10.1021/acs.est.8b05318, 2019.

Weiss, R. F.: The solubility of nitrogen, oxygen and argon in water and seawater, Deep Sea Res. Oceanogr. Abstr., 17, 721–735, https://doi.org/10.1016/0011-7471(70)90037-9, 1970.